Eur. Phys. J. D (2015)
DOI: 10.1140/epjd/e2014-50798-5

THE EUROPEAN PHYSICAL JOURNAL D

Regular Article

Numerical study of the dispersion characteristics of a semi-circularly corrugated slow wave structure

Md. Ghulam Saber[a], Rakibul Hasan Sagor, and Md. Ruhul Amin

Department of Electrical and Electronic Engineering, Islamic University of Technology (IUT), Board Bazar, Gazipur-1704, Bangladesh

Received 7 November 2014 / Received in final form 4 December 2014
Published online (Inserted Later) – © EDP Sciences, Società Italiana di Fisica, Springer-Verlag 2015

Abstract. The dispersion characteristics of the axisymmetric transverse magnetic (TM) modes of a semi-circularly corrugated periodic metallic slow wave structure (SCCSWS) have been analysed numerically by approximating the axial profile of the SWS using Fourier series. The theoretical results and some of their representative experimental counterpart revealed that, instead of using complex boundary conditions, the Fourier approximation of the axial profile can be used in deriving the dispersion relation using linear Rayleigh-Fourier (R-F) theory. An analytical equation has been derived in order to determine the Fourier constants of the approximated axial profile. Numerical technique has also been employed to calculate the Fourier constants. The dispersion relation for the SCCSWS is analysed for the cold structure which is characterized by the real value of frequency and wavenumber. The dispersion characteristics of the fundamental as well as higher order TM modes have been calculated using Fourier constants obtained by both analytical and numerical techniques. The SCCSWS analysed in this paper can be implemented in real experiments for the generation of high-power microwaves.

1 Introduction

Backward wave oscillators (BWO) are high power microwave devices which are designed to transform the electron beam energy into electromagnetic radiation at microwave frequencies [1,2] of the electromagnetic spectrum. An O-type BWO comprises of an axially propagating electron beam through a resonant cavity consisting some kind of slow wave structure (SWS) bounded by a strong magnetic field. Metallic cylinders with periodically corrugated inner wall are being extensively used as SWSs in BWOs. The SWSs are designed to slow down the electromagnetic wave with phase velocities less than the speed of light so that it can resonantly interact with the electron beam. This resonant interaction leads to an instability which is the prerequisite of energy transfer from the electron beam to the electromagnetic wave. The BWO has been named so because it operates in the negative group velocity regime and periodic SWSs are necessary for obtaining negative group velocity [3,4].

During the earlier days of development of the BWOs, dielectric loaded periodic structures were used as the SWS. However, this kind of structure cannot support high power because of the problem of dielectric breakdown. Use of intense relativistic electron beam generates a very high electric field inside the structure which causes this breakdown. In order to get rid of this alarming problem metallic hollow waveguides with periodically corrugated inner walls are now being used as the SWS [5–10]. Among different corrugation profiles the sinusoidally corrugated SWS (SCSWS) has achieved the greatest attention of the researchers [11–17]. Although the SCSWS has some advantages, it is difficult to fabricate a sinusoidal profile in the inner wall of a metallic waveguide. Many researchers have reported some viable alternative periodic profiles such as trapezoidal corrugation [6,18], rectangular corrugation [7,19], doubly rippled inner wall [20], etc. In this paper, we propose a semi-circularly corrugated SWS (SCCSWS) as a substitute of the SCSWS. The axial profile of the SCCSWS has been approximated using Fourier series which allows the use of simple R-F theory for the analysis of the cold structure dispersion characteristics which have only real roots for eigen modes. This method has already been applied successfully both numerically [6] and experimentally [18].

The Fourier constants of the approximated axial profile have been determined using both analytical and numerical approach. The TM_{01}-TM_{04} modes have been determined using the obtained Fourier constants and compared. Convergence tests have been performed to ensure the accuracy of the obtained results. We have also determined the fundamental and higher order TM modes by varying the periodicity of the SCCSWS. To the best of our knowledge, this is the first time one has analysed the beam free dispersion characteristics of the SCCSWS so rigorously.

The organization of the paper is as follows: Section 2 depicts the mathematical summary of the derivation of

[a] e-mail: gsaber@iut-dhaka.edu

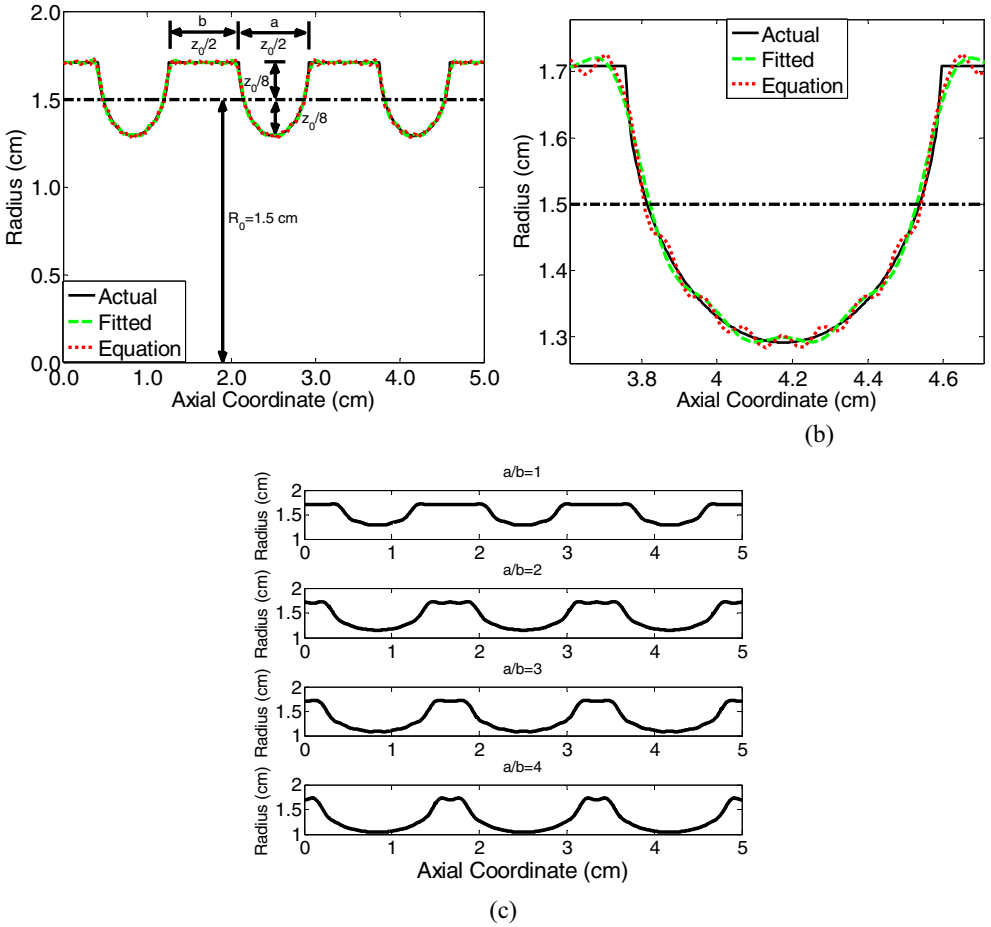

Fig. 1. (a) Axial profile of the axisymmetric SCCSWS. Black solid line indicates the ideal semi-circular profile, green dashed line indicates the fitted profile using Fourier constants obtained utilizing numerical technique and red dashed line indicates the axial profile drawn using Fourier constants obtained using the derived equation. (b) Magnified profile for one semi-circle. (c) Axial profile for different duty ratios (a/b).

Table 1. Fourier approximation of the SCCSWS using analytical and numerical techniques.

Type of SWS	$R(z)$
Semi-circular equation	$R(z) = \left(R_0 + \frac{Z_0}{8}\right) + \left[\frac{Z_0}{8} + \frac{Z_0}{2\pi}\sum_{n=1}^{\infty}\frac{(-1)^n J_1(n\pi)}{n}\cos\left\{n\pi\left(\frac{4z}{Z_0}+1\right)\right\}\right] \times \left[\sum_{n=1}^{\infty}\frac{1}{(2n-1)}\sin\left\{(2n-1)\left(\frac{2z}{Z_0}+\frac{1}{2}\right)\pi\right\} - \frac{\pi}{4}\right]$
Semi-circular	$R(z) = R_0 + \sum_{v=1}^{\infty} A_v\cos(vk_0z) + B_v\sin(vk_0z)$, A and B constants are obtained numerically

the dispersion relation, numerical results are presented in Section 3 and Section 4 presents the discussion and conclusion.

2 Mathematical modeling

A representative section of the proposed SCCSWS is given in Figure 1a and it has been magnified for one semi-circle in Figure 1b. We have determined the dispersion characteristics for different values of the ratio (a/b) of the axial profile. Figure 1c depicts the axial profile for different periodic ratio of the SCCSWS. We have chosen the size parameters of the SCCSWS such that it operates in X-band frequency range.

The axial variation of the radial function $R(z)$ makes the structure periodic. For SWS with simpler corrugation such as, rectangular, triangular or trapezoidal, $R(z)$ can be determined easily. However, for the SCCSWS, it is difficult to obtain Fourier constants analytically. In this case, numerical techniques are used to find the Fourier constants. We have also derived an analytical equation to represent the axial profile in terms of the Fourier series. Table 1 depicts both analytical and numerical Fourier expression of $R(z)$ for the SCCSWS, where, R_0 is the average

radius, h is the corrugation amplitude, $k_0 = 2\pi/z_0$ and z_0 is the period of corrugation, J_1 is the first order Bessel function of the first kind and the integer v is the harmonic number.

In case of cold structure the EM field components of the TM modes of the structure can be expressed by an infinite sum of the Floquet harmonics as:

$$E_z(r,z,t) = \sum_{n=-\infty}^{\infty} E_{zn}(r) e^{i(k_{zn}z-\omega t)} \tag{1}$$

where, $k_{zn} = k_z + nK_0$ an $n = 0, \pm1, \pm2, \ldots$ is the Floquet harmonic number and k_z is the axial wavenumber.

Transverse variation of E_{zn} can be obtained using,

$$\frac{1}{r}\frac{d}{dr}\left(r\frac{dE_{zn}}{dr}\right) + \beta_n^2 E_{zn} = 0 \tag{2}$$

where, $\beta_n^2 = (\omega/c)^2 - k_{zn}^2$ is the square of transverse wavenumber, c is the velocity of light in vacuum and the general solution of (2) can be written as,

$$E_{zn}(r) = A_n J_0(\beta_n r) \tag{3}$$

where J_0 is the 0th order Bessel's function of the first kind.

The transverse electric field component is given by:

$$E_{rn} = \frac{ik_{zn}}{\beta_n^2}\frac{dE_{zn}}{dr} \tag{4}$$

where n is the Floquet harmonic number.

The tangential field components of the electric field to the inner wall of the SWS must vanish if we assume that the inner wall is a perfect conductor. Each spatial harmonics of the fields inside the SWS will satisfy the boundary condition. The vector tangent to the inner wall of the SWS is $\vec{t} = \vec{r}\frac{dr(z)}{dz} + \vec{z}$, so the boundary condition can be expressed as [4,5],

$$E_t \propto \left| E_z + \sum_{n=-\infty}^{\infty} \frac{ik_{zn}}{\beta_n^2}\frac{dE_{zn}}{dr}\frac{dR(z)}{dz}\right|_{r=R(z)} = 0. \tag{5}$$

By multiplying (5) with $\exp(-imK_0 z)$ and integrating it over one period of the SWS ($z = -\frac{z_0}{2}$ to $z = \frac{z_0}{2}$) the dispersion relation can be obtained. This operation is essentially equivalent to expanding each term in the sum of (5) in a spatial Fourier series.

$$\sum_{m,n=-\infty}^{\infty} A_n \int_{-\frac{z_2}{2}}^{\frac{z_2}{2}} e^{i(n-m)K_0 z}\left(1 + \frac{ik_{zn}}{\beta_n^2}\frac{d}{dz}\right) \times [J_0(\beta_n r)]\, dz = 0 \tag{6}$$

at $r = R(z)$.

Equation (6) can be expressed in a concise form as:

$$\sum_{m,n=-\infty}^{\infty} A_n [1 + (m-n)Q_n] P_{mn}^J = \sum_{m,n=-\infty}^{\infty} D_{mn} A_n = 0 \tag{7}$$

Table 2. The size parameters of the SCCSWS.

Parameter	R_0 (cm)	z_0 (cm)	K_0 (cm^{-1})
SCCSWS	1.50	1.67	3.76

where

$$Q_n = \frac{K_0 k_{zn}}{\beta_n^2}, \quad D_{mn} = [1 + (m-n)Q_n]\left(P_{mn}^J\right),$$

$$P_{mn}^J = \int_0^{\pi} \cos[(n-m)u]\, J_0(\beta_n R(z))\, du \quad \text{and} \quad u = K_0 z.$$

In equation (7) A_n is a column matrix represents the amplitude of Floquet harmonics. The dispersion relation results from the fact that in the solution of (7), at least some $A_n \neq 0$. This implies that

$$\det\left[\sum_{m.n=-\infty}^{\infty} D_{mn}\right] = 0. \tag{8}$$

Equation (8) is the required generalized bream free dispersion relation for the corrugated SWS. Different axial profile can be studied using this relation by choosing the required expression for $R(z)$ in the integration. The determinant D_{mn} is a function of f and k. Though the rank of the determinant is infinite, we must truncate it to a finite value for practical application. If we consider that the number of Floquet harmonics $n(=N)$ is equal to the number of Fourier harmonics $m(=N)$, then n and m in D_{mn} are bounded to $-\frac{(N-1)}{2} \leqslant n, m \leqslant \frac{(N-1)}{2}$ if we assume that the number of Floquet harmonics equals the number of Fourier harmonics. Thus we obtain a rank of $2N$ for the determinant. A trade-off is made on the value of N to obtain converged dispersion characteristics.

Table 2 depicts the chosen structure size parameters for operation in the X-band. We have used Gauss' quadrature integration formula to determine P_{mn}^J and the Newton-Raphson method to solve the determinant D_{mn}. Results are presented in the subsequent sections.

3 Numerical results

The Fourier constants of the Fourier series approximated axial profile of the proposed SCCSWS have been determined using both analytical and numerical techniques. We have also varied the period of the corrugation in the SCCSWS and obtained the Fourier constants for those cases utilizing numerical technique. The axial profiles of the SCCSWS for different values of ratio a/b are presented in Figure 1c. The goodness of the Fourier coefficients obtained using numerical method has been tested utilizing different statistical indices such as sum of squared errors of prediction (SSE), R-square, root mean squared error (RMSE) and adjusted R-square and presented in Table 3. This has been done in order to ensure the accuracy of our obtained results.

Table 3. Goodness of the Fourier fit using numerically obtained Fourier constants.

No. of Fourier harmonics	a/b	SSE	R-square	RMSE	Adjusted R-square
8	1	0.1436	0.9962	0.01100	0.9961
8	2	0.2057	0.9967	0.01319	0.9967
8	3	0.2507	0.9965	0.01456	0.9965
8	4	0.2158	0.9971	0.01351	0.9971

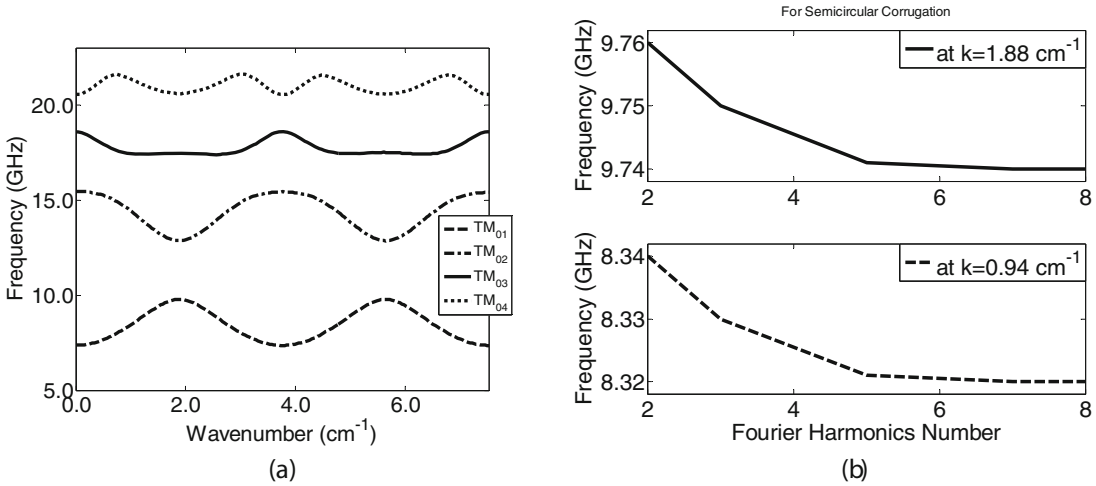

Fig. 2. (a) Fundamental and higher order TM modes of SCCSWS for two periods. The size parameters are given in Table 2. (b) Test of convergence of oscillation frequency for different Fourier harmonic number for SCCSWS.

3.1 Dispersion curve of fundamental and higher order TM modes for zero beam current

In order to validate the numerically calculated dispersion characteristics of the TM modes, the convergence of the obtained results have been tested first by several methods. The first method used to determine the convergence is by testing the periodicity $f(k_z + nK_0) = f(k_z)$ of the dispersion diagram in f-k plane. We have determined the dispersion diagrams for TM_{01}-TM_{04} modes for $k = 2 \times 3.76$ cm^{-1} and the curves are depicted in Figure 2a. The periodicity is perfectly maintained over the 2 periods for all four TM modes.

Though the Fourier series contains infinite number of harmonics, we need to truncate it to a practically feasible finite number. We found that eight harmonics provide reasonably accurate results for our case. Figure 2b depicts the frequency for different Fourier harmonics number taken at $k = 0.94$ cm^{-1} and $k = 1.88$ cm^{-1} for our proposed SCCSWS. It can be observed that for 6, 7 and 8 Fourier harmonics the frequency at those two particular wavenumbers is almost constant. Thus it is evident that taking eight Fourier harmonics is enough for the results to be accurate.

The O-type Cherenkov devices such as BWOs operate at a frequency and wavenumber which can be roughly estimated from the intersecting points of the beam lines and the dispersion curve. It is important to understand the dispersion properties of the SWS in order to approximate the operating frequency of the BWO before real experiment. Hence we begin by investigating the dispersion relation of the SCCSWS for the cold structure. In O-type Cherenkov devices two key parameters of the SWS play predominant role in determining the frequency, which are mean radius of the SWS structure, r_0 and the period of variation of the inner wall radius, z_0. In case of zero beam current, the dispersion relation of the cold SCCSWS is exact and the structure can be assumed to be infinitely long.

Figure 3a depicts the dispersion curve for TM_{01} mode along with the light line and the beam lines for different beam energies. The dispersion curve has been determined by the R-F method using the numerically obtained Fourier constants. As it has been already mentioned that we can approximate the expected oscillation frequency from the intersection of dispersion curve and beam lines, we have determined the frequencies at the intersecting points and presented them in Table 4. As the value of β is decreased, the beam line shifts to right and the oscillation frequency decreases. The beam space charge wave can interact with any of the TM modes of the structure in case of real experiments if other conditions are met. We have compared the dispersion curves for the fundamental and the higher order TM modes calculated using both numerically and analytically obtained Fourier constants which are presented in Figure 3b. A very good agreement can be observed for the fundamental TM mode; however, the difference between the dispersion curves becomes more prominent as we go for higher order modes. This can be explained from the fact that the axial profile achieved using Fourier constants

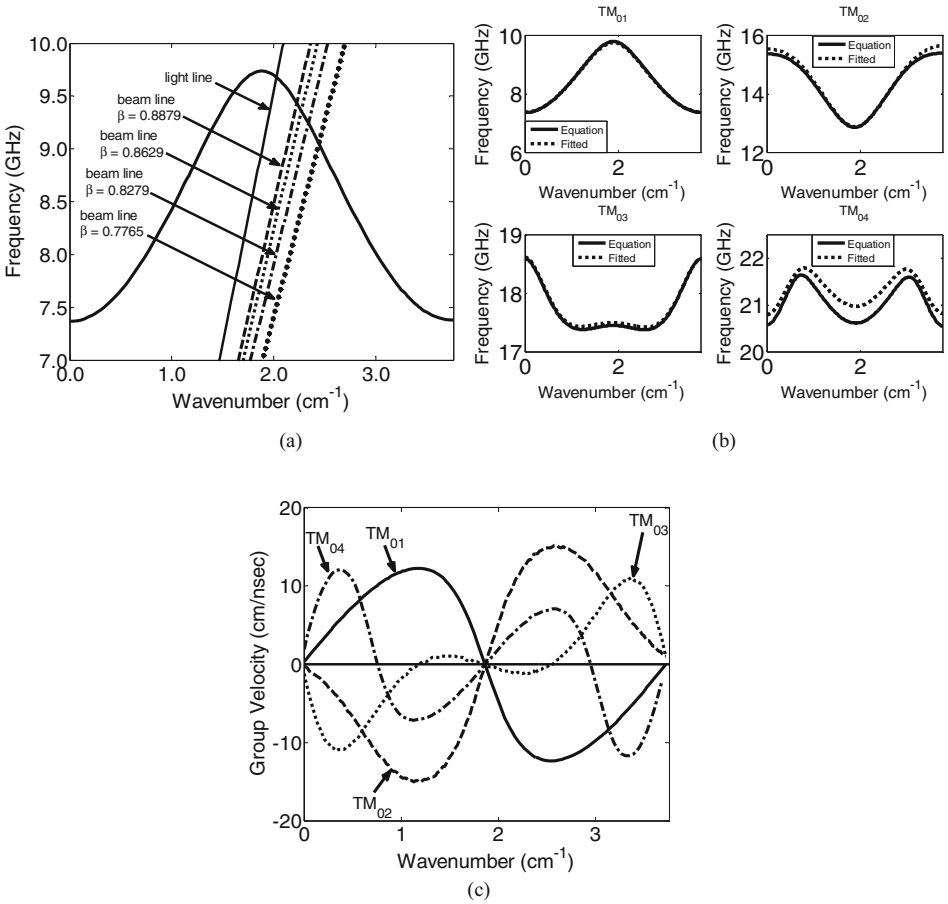

Fig. 3. (a) TM_{01} mode dispersion curves for SCCSWS with light line and beam lines for different beam energy. (b) Comparison of the fundamental and higher order TM modes obtained for Fourier approximation done using equation and numerical technique for SCCSWS. (c) The group velocities for the four TM modes.

Table 4. Resonant frequency and group velocity of the axial TM_{01} mode of SCCSWS for different beam energy.

V_b (KV)	γ	β	f (GHz)	Wavenumber (cm^{-1})	v_g (cm/ns)
		Light line	9.697	2.031	–5.70
600	2.1742	0.8879	9.407	2.219	–10.06
500	1.9785	0.8629	9.375	2.275	–10.86
400	1.7828	0.8279	9.217	2.351	–11.63
300	1.5871	0.7765	9.064	2.445	–12.18

obtained with analytical and numerical approach does not coincide perfectly as presented in Figure 1b.

The speed of the axial energy transport by the structure modes is determined by group velocity, v_g which is calculated by taking the derivative of the dispersion equation:

$$v_g = \frac{d\omega}{dk}. \tag{9}$$

The group velocities for the first four TM modes have been determined and depicted in Figure 3c. The corresponding wavenumbers of the intersecting points of the light line and the beam lines and the dispersion curve of TM_{01} mode is calculated from Figure 3a. When we observe the group velocities at those wavenumbers, we find that they represent the negative group velocity region which corresponds to the operating regime of an O-type BWO. The group velocities at those wavenumbers are presented in Table 4.

3.2 Dispersion curves for different values of the ratio a/b

Dispersion curves of fundamental and higher order TM modes for different values of the ratio a/b are depicted in Figures 4a–4c. The light line and the beam lines are also drawn for TM_{01} mode. As we decrease the periodic ratio (a/b), the SCCSWS gets the shape of a smooth cylindrical waveguide and the cut-off frequency increases for TM_{01} mode. Thus we can infer that the TM_{01} mode cut-off frequency can be tuned by varying the periodic ratio and is inversely proportional to it. This is consistent with

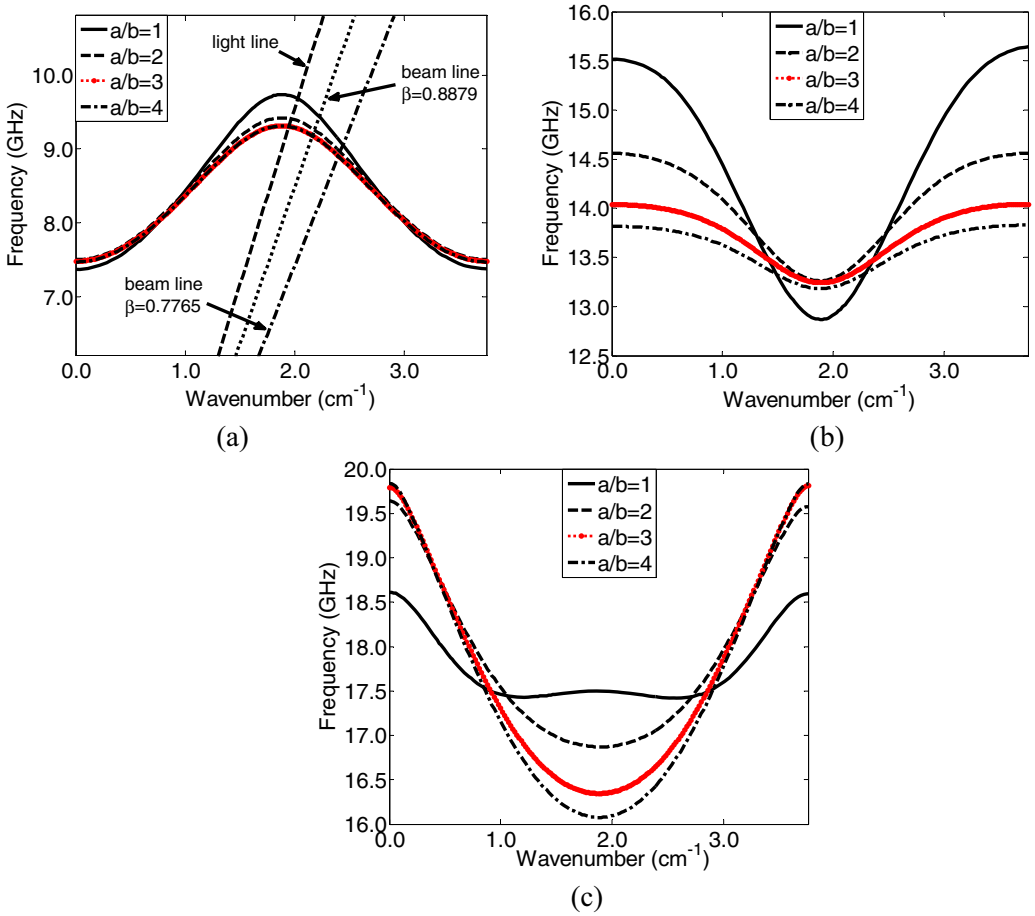

Fig. 4. Dispersion curves for various values of a/b ratio (a) TM_{01} mode with light line and beam lines. (b) TM_{02} mode. (c) TM_{03} mode.

Table 5. Resonant frequency of the axial TM_{01} mode of SCCSWS for different periodic ratio and beam energy.

V_b (KV)	β	f (GHz)			
		$a/b=1$	$a/b=2$	$a/b=3$	$a/b=4$
	Light line	9.675	9.42	9.045	9.039
600	0.8879	9.404	9.245	8.946	8.941
300	0.7765	9.300	9.170	8.894	8.891

the theory since we know that the period of variation of the axial profile, z_0 is one the key factors that influence the dispersion relation. The frequencies at the intersecting points of light line and beam lines with the dispersion curves for different periodic ratios are presented in Table 5. High-frequency operation of the device could be possible for the same beam energy for smaller values of the periodic ratio. The variation of dispersion curves for TM_{02} and TM_{03} modes with the variation of periodic ratios are depicted in Figures 4b and 4c.

4 Discussion and conclusion

The zero beam current dispersion properties of a novel X-band SCCSWS is studied and presented. Our treatment has included both analytical and numerical approach for the determination of the Fourier constants of the axial profile. The dispersion properties of the proposed axially varying SWS have been determined using the R-F method. The dispersion relation of a cold SWS permits only real values of ω when solved as a function of real k. The resulting linear dispersion relations allow us to approximate the oscillation frequency of the device qualitatively as a function of the axial wavenumber. An essential agreement has been observed between the dispersion curves calculated using analytically and numerically obtained Fourier constants. It can be concluded that the proposed novel SCCSWS can be deployed in real BWO experiments as a viable alternative of other types of SWS such as sinusoidally corrugated SWS which is very difficult to be constructed precisely [21].

Appendix

Table A.1. Numerically obtained Fourier constants for different values of the ratio a/b (As and Bs are in cm).

$a/b = 1$	$a/b = 2$	$a/b = 3$	$a/b = 4$
$A0 = 1.545$	$A0 = 1.419$	$A0 = 1.342$	$A0 = 1.293$
$A1 = 0.2366$	$A1 = 0.3161$	$A1 = 0.3318$	$A1 = 0.3306$
$B1 = -0.0007977$	$B1 = -0.0003379$	$B1 = -0.001288$	$B1 = -0.0001186$
$A2 = -0.05966$	$A2 = 0.03577$	$A2 = 0.08695$	$A2 = 0.1091$
$B2 = 0.0004029$	$B2 = -7.621\text{E-}05$	$B2 = -0.0006743$	$B2 = -7.825\text{E-}05$
$A3 = -0.03903$	$A3 = -0.04047$	$A3 = 0.00176$	$A3 = 0.03028$
$B3 = 0.0003945$	$B3 = 0.00013$	$B3 = -1.902\text{E-}05$	$B3 = -3.246\text{E-}05$
$A4 = 0.02231$	$A4 = -0.03725$	$A4 = -0.02864$	$A4 = -0.006919$
$B4 = -0.0003016$	$B4 = 0.0001591$	$B4 = 0.000446$	$B4 = 1.011\text{E-}05$
$A5 = 0.0175$	$A5 = -0.006997$	$A5 = -0.02915$	$A5 = -0.02177$
$B5 = -0.0002945$	$B5 = 3.695\text{E-}05$	$B5 = 0.0005658$	$B5 = 3.921\text{E-}05$
$A6 = -0.01239$	$A6 = 0.015$	$A6 = -0.01528$	$A6 = -0.02262$
$B6 = 0.0002515$	$B6 = -9.658\text{E-}05$	$B6 = 0.0003547$	$B6 = 4.874\text{E-}05$
$A7 = -0.01037$	$A7 = 0.0158$	$A7 = 0.0006623$	$A7 = -0.01554$
$B7 = 0.0002442$	$B7 = -0.0001181$	$B7 = -2.006\text{E-}05$	$B7 = 3.893\text{E-}05$
$A8 = 0.00814$	$A8 = 0.002898$	$A8 = 0.01069$	$A8 = -0.005653$
$B8 = -0.0002204$	$B8 = -2.431\text{E-}05$	$B8 = -0.0003334$	$B8 = 1.604\text{E-}05$
$K_0 = 3.760\ \text{cm}^{-1}$	$K_0 = 3.762\ \text{cm}^{-1}$	$K_0 = 3.761\ \text{cm}^{-1}$	$K_0 = 3.762\ \text{cm}^{-1}$

References

1. R.G. Hutter, S.W. Harrison, *Beam and Wave Electronics in Microwave Tubes*, 1st ed. (D. Van Nostrand, New York, 1960)
2. J.E. Rowe, *Nonlinear Electron-wave Interaction Phenomena* (Academic Press, 1965)
3. C. Elachi, Proc. IEEE **64**, 1666 (1976)
4. J. Benford et al., *High Power Microwaves* (CRC Press, 2007)
5. M. Amin, K. Ogura, Microw. Antennas Propag. IET **1**, 575 (2007)
6. M.R. Amin, K. Ogura, IEEE Trans. Plasma Sci. **41**, 2257 (2013)
7. K. Ogura et al., IEEE Trans. Plasma Sci. **41**, 2729 (2013)
8. N. Ginzburg et al., Phys. Rev. E **60**, 3297 (1999)
9. S.D. Korovin et al., IEEE Trans. Plasma Sci. **28**, 485 (2000)
10. G. Burt et al., Phys. Rev. E **70**, 046402 (2004)
11. R.A. Kehs et al., IEEE Trans. Plasma Sci. **13**, 559 (1985)
12. J.A. Swegle et al., Phys. Fluids **28**, 2882 (1985)
13. K. Minami et al., IEEE Trans. Plasma Sci. **30**, 1134 (2002)
14. F.D. Kantrowitz, E.A. Adler, Plasma Sci. IEEE Trans. **37**, 2619 (1990)
15. J.J. Barroso et al., IEEE Trans. Plasma Sci. **31**, 752 (2003)
16. T. Watanabe et al., Phys. Rev. E **69**, 056606 (2004)
17. H. Yamazaki et al., J. Plasma Fusion Res. Ser. **6**, 719 (2004)
18. M.R. Amin et al., IEEE Trans. Plasma Sci. **42**, 1495 (2014)
19. K. Ogura et al., Plasma Fusion Res. **9**, 3406022 (2014)
20. M.R. Amin, IET Microw. Antennas Propag. **7**, 105 (2013)
21. M.R. Amin et al., J. Phys. Soc. Jpn **64**, 4473 (1995)